Reelin Immunoreactivity in the Adult Primate Brain: Intracellular Localization in Projecting and Local Circuit Neurons of the Cerebral Cortex, Hippocampus and Subcortical Regions

Verónica Martínez-Cerdeño, María José Galazo, Carmen Cavada and Francisco Clascá

Department of Morphology, School of Medicine, Autónoma University, Madrid, Spain

Reelin is a large secretable protein which is widely expressed by specific neuronal populations. In the embryonic brain, Reelin plays a signaling role critical for the correct positioning of migrating neuroblasts. Reelin is also expressed in the adult mammalian brain, including humans; however, its function/s there remain poorly understood. To gain insight into which neuronal populations and specific circuits may be influenced by Reelin in the adult, we have conducted a light and electron microscope analysis of Reelin-immunoreactive neuron types in the cerebral cortex and subcortical regions of adult macaque monkeys. Results show that the great majority of brain neurons, including interneurons and projection neurons, are immunoreactive for Reelin although some neuronal populations do not contain Reelin. The immunoreactive protein is located intracellularly, mainly in neuronal somata. Reelin is also present in gray matter neuropil as well as in some long axonal pathways and their terminal arborizations, suggesting that it can be axonally transported over long distances. The staining patterns in the labeled neurons are remarkably diverse. Our observations reveal a wider distribution of Reelin in the adult macaque brain than in any other species investigated to date. The data show that Reelin is in a position to influence most brain circuits in the adult primate brain.

Introduction

Reelin is the protein product of the mutated gene in *reeler* mice (D'Arcangelo *et al*., 1995; Ogawa *et al*., 1995), a strain characterized by ataxic gait and widespread disruption of neuronal positioning in the central nervous system (Caviness *et al*., 1988; Phelps *et al*., 2002). Recently, the Reelin gene has also been found to be mutated in a recessive form of human lissencephaly with cerebellar hypoplasia (Hong *et al*., 2000). Reelin is a large secretable protein (385 kDa), but shorter forms arise via cleavage of full-length Reelin into two smaller proteins of ~250 and 180 kDa (Lambert de Rouvroit *et al*., 1999). All forms contain an N-terminal domain that is similar to F-spondin (De Bergeyck *et al*., 1998), a protein that is secreted by floor plate cells and that directs neuronal migration and axonal growth in the spinal cord (Klar *et al*., 1992). Evidence accumulated in recent years indicates that, during development, Reelin is involved in the control of neuroblast positioning through regulation of cell-to-cell adhesion. The proposed mechanisms involve Reelin acting as an intercellular signaling molecule of the extracellular matrix [for recent reviews see Rice and Curran (Rice and Curran 2001), or Aboitiz *et al*. (Aboitiz *et al*., 2001)]. Reelin has been shown to be secreted (Miyata *et al*., 1996; D'Arcangelo *et al*., 1997; Lacor *et al*., 2000; Jossin and Goffinet, 2001), and bind to receptors (D'Arcangelo *et al*., 1999; Hiesberger *et al*., 1999; Dulabon *et al*., 2000). The Reelin signal can then be transduced in target cells by several putative pathways (Rice and Curran, 2001). A wealth of genetic data, as well as *in vitro* and *in vivo* experiments, support the view that such mechanisms may be at work, for example, in the genesis of the inside-out neurogenetic gradient of the cerebral cortex (Gleeson and Wash, 2000; Rice and Curran, 2001; Magdaleno *et al*., 2002).

In addition, substantial amounts of Reelin protein or mRNA have also been found in the adult brain (Schiffmann *et al*., 1997; Alcántara *et al*., 1998; Impagnatiello *et al*., 1998; Pesold *et al*., 1998, 1999; Guidotti *et al*., 2000; Rodríguez *et al*., 2000) as well as other body tissues (Hong *et al*., 2000; Smalheiser *et al*., 2000; Heymann *et al*., 2001) of mammals, including humans. Nevertheless, the biological function/s of Reelin in the adult brain remain poorly understood. The observation that Reelin is associated to integrin receptors in dendrites led to the suggestion that it may be involved in the modulation of synaptic plasticity (Pesold *et al*., 1998, 1999; Rodríguez *et al*., 2000; Quattrocchi *et al*., 2002).

We reasoned that insight into the neuronal populations and specific circuits that contain Reelin in the adult brain could yield valuable clues regarding Reelin function after development. The available data were fragmentary and largely based on rodent material (Miyata *et al*., 1996; Alcántara *et al*., 1998; Pesold *et al*., 1998, 1999). Data on primates, including humans, are limited to samples from a few cortical areas (Impagnatiello *et al*., 1998; Fatemi *et al*., 2000; Guidotti *et al*., 2000; Rodríguez *et al*., 2000; Pérez-García *et al*., 2001; Zecevic and Rakic, 2001). In general, these studies have reported that, in the cerebral cortex, Reelin is localized to specific interneuron populations, prominently in layer I. However, a systematic study of Reelin protein in cortical and subcortical structures of the primate brain has not yet been published. Consequently, we set out to analyze Reelin-immunoreactivity in cortical and subcortical regions of adult macaques at the light and electron microscope levels.

Results show that a very large majority of brain, cerebellum and brainstem neurons, including both interneurons and projection neurons, are immunoreactive for Reelin in adult macaques. The epitopes detected by the antibodies used in this study are located intracellularly, mainly in neuronal somata and proximal dendrites. In addition, Reelin-like immunoreactivity is present in the neuropil of most gray matter areas, as well as in some axonal pathways and their terminal arborizations. It follows from our results that Reelin distribution is more widespread in the brain of adult primates than in any other mammalian order investigated to date. Overall, our data are consistent with the notion that, in the adult, Reelin may be involved in the modulation of synaptic plasticity; moreover, they suggest that this modulatory role is remarkably prevalent in the primate brain.

Materials and Methods

Tissue Fixation

Brain tissue from a total of six adult macaques (four males and one female *Macaca nemestrina*, and one adult female *Macaca mulatta*) was used for the present study. All procedures involving these animals were carried out in accordance with European Community Council Directive

86/609/EEC guidelines. All animals were killed with sodium pentobarbital (80 mg/kg) immediately before fixation.

Two animals were first perfused through the left ventricle with saline (5 min), followed by 4% paraformaldehyde in 0.1 M phosphate buffer pH 7.4 (PB) for 1 h. In the remaining four animals, the fixative solution used after the saline contained 4% paraformaldehyde + 0.15–0.2% glutaraldehyde in PB. In all cases, excess fixative was subsequently flushed by perfusion with a graded series of sucrose solutions (5%, 15% and 30%) in PB at 4°C. Once perfusion was completed, brains were stereotaxically split in coronal blocks, and removed from the skull.

Freeze Sectioning

Tissue blocks from five animals were cryoprotected by soaking in a 30% sucrose solution in PB until they sank. Parallel series of 50 μm thick coronal sections were then obtained on a freezing microtome. For cytoarchitectonic reference, one series of sections was mounted onto gelatin-coated glass slides, air-dried, stained with cresyl violet, dehydrated and coverslipped. Other series of sections from which the present material was taken were soaked in a buffered 20% ethylenglycol solution and stored at –20°C.

Immunohistochemistry for Light Microscopy

Prior to beginning the immunohistochemical protocol, a series of three to eight coronal sections that as a group covered a variety of rostrocaudal levels of the brain and brainstem were selected from each brain. Sections included samples from a wide variety of coronal levels across the cerebral hemispheres, thalamus, hypothalamus, mesencephalon, pons, rostral medulla oblongata and cerebellum; the olfactory bulbs were not included.

Sections were thoroughly rinsed in PB at 4°C for 48 h. Sections were then pretreated with a 1% hydrogen peroxide solution in phosphate-buffered saline (PBS) solution for 20 min, rinsed, and subsequently blocked with 10% horse serum + 3% bovine serum albumin + 0.5% Triton X-100 in 0.1 M PBS. Sections were incubated for 48 h at room temperature, either in mouse monoclonal IgG 142 (1:400, a gift of Dr A.M. Goffinet, Namur, Belgium), or mouse monoclonal IgG CR-50 (1:400 a gift of Dr M. Ogawa, RIKEN, Japan). A biotinylated horse anti-mouse IgG (Pierce, Rockford, IL, 1:200) was used as secondary antibody. Immunoreagents were diluted in 0.1 M PBS containing 3% normal horse serum and 0.1% Triton X-100. Sections were subsequently incubated in avidin–biotinylated horseradish peroxidase complex (ABC, Vector Laboratories, Burlingame, CA) in 0.1 M PBS for 1 h, and developed with 0.01% H_2O_2 + 0.04% 3,3′-diaminobenzidine tetrahydrochloride (DAB) in acetate buffer pH 6. In some experiments, we enhanced the opacity of the reaction product by including 2.5% nickel sulfate in the developer medium (Ni-DAB). Multiple rinses in PBS were performed between each of the above steps. The specificity of the monoclonal antibodies used is well characterized (De Bergeyck *et al.*, 1998). In addition, each experiment included a control section processed without the primary antibodies and this always resulted in the absence of immunostaining. The concentration of primary antibodies was tested and optimized in preliminary experiments.

Sections were mounted on gelatin-coated glass slides and air-dried. Some sections were lightly counterstained with cresyl violet. All sections were finally dehydrated in graded alcohols, cleared in xylene, and coverslipped with DePeX.

Semithin Tissue Sections

After removal from the skull, tissue blocks from the sixth animal (a male *nemestrina* macaque perfused with the aldehyde mixture that included 0.2% glutaraldehyde, see above) were cryoprotected by soaking in 20% glycerol in PB. The tissue blocks were then stored at –20°C for several months. Forty-eight hours prior to beginning the immunohistochemical staining protocol, small (~300 mm^3) tissue portions were dissected. These portions included samples of the isocortex (rostral prefrontal cortex, striate cortex), the hippocampal formation, the head of the caudate nucleus, and some cerebellar folia. The portions were rinsed in phosphate buffer for 12 h at 4°C and subsequently vibrosliced at 40 μm.

Sections underwent pre-embedding immunostaining following a protocol equivalent to the one described above, except for the absence of Triton X-100 in all steps. The sections were briefly mounted in PBS onto glass slides and examined under the light microscope. Although consistent, the immunolabeling was weaker than that obtained using Triton X-100. Regions of interest were then dissected from the section, postfixed in osmium tetroxide (2% in 0.1 M cacodylate buffer), dehydrated, and flat-embedded in Araldite. Serial semithin (2–3 μm) sections were cut from these samples on a Reichert Ultracut ultramicrotome. Semithin sections were counterstained with toluidine blue, mounted on glass slides, and dry-coverslipped.

Light Microscopy Analysis

Thick (40–50 μm) and semithin (2–3 μm) sections were examined in a Nikon Eclipse microscope at 40–1000× under bright and dark-field illumination. Resolving the various cell-specific patterns of immunolabeling required the systematic use of 1000× oil-immersion optics for each investigated brain region.

Ultrathin Re-sectioning and Electron Microscopy

Cells with identifiable cellular morphology and evident Reelin immunostaining were selected (n = 16) from the semithin sections. These cells were photographed and their location recorded on detailed camera lucida drawings. Under a stereomicroscope, the tissue region (~2 mm^2) containing each cell was then dissected, flat-mounted in Araldite, and re-sectioned in ultrathin (60–80 nm) sections. Some ultrathin sections were intensified with lead citrate (0.4%), while other sections were left without intensification. Sections were visualized at 1000–100 000× using a JEOL JEM 1010 transmission electron microscope. Sections were imaged for analysis with a Bioscan digital imaging system (Gatan, Pleasanton, CA, USA). For the purpose of illustration, the regions of interest were directly photographed on film.

Results

Every cortical field and subcortical structure that we examined contained large numbers of immunoreactive neuronal somata. Some non-immunoreactive neurons were also present in most regions. In addition, we observed a fine-grained immunoprecipitate in the gray matter neuropil of these regions, as well as in some specific axonal tracts. No labeling was observed in glial, pial or endothelial cells. Immunostaining with either of the two monoclonal anti-Reelin IgGs assayed (142 and CR-50) resulted in similar staining, although CR-50 yielded a weaker staining and higher background. Immunostaining in all six experimental cases was consistent; however, it was most intense in the two brains that had been fixed without glutaraldehyde. Our observations are summarized in Table 1.

General Features and Distribution of the Reelin-immunoreactive Neuronal Somata

Throughout the brain, immunolabeled neuronal somata displayed a wide spectrum of staining patterns and intensities with one of two basic staining patterns generally being present: (a) labeled particles located in the cell soma (PReln-ir neurons), or (b) a solid stain that cleanly labeled the perikaryon and, often, the first- and second-order dendrites as well (SReln-ir neurons). Although some cells showed intermediate features and were difficult to classify, we found these categories generally consistent and useful for descriptive purposes.

The relative number and distribution of PReln-ir neurons and SReln-ir neurons was markedly dissimilar across brain regions. The PReln-ir neurons were the great majority in all the examined structures, while SReln-ir neurons were notably less numerous, and largely limited to telencephalic structures (Table 1). Nevertheless, the superficial layer of the cerebral cortex (layer I in the isocortex, or the molecular strata in the hippocampal formation and olfactory areas) contained almost no PReln-ir neurons although it did contain a large population of SReln-ir neurons (Figs 1 and 2).

At low magnification, staining looked ‘weak’ in the PReln-ir

Table 1

Localization and relative proportion of Reelin-immunoreactive neuronal somata and neuropil in cortical and subcortical regions of the adult macaque brain

		Neuronal somata with solid labeling (**SReln-ir cells**)	Neuronal somata with particulated labeling (**PReln-ir cells**)	Immunoreactive neuropil
Isocortex *				
Layer I		●●	○	++
Layer II		●	○○	+
Layer III		•	○○	+
Layer IV		•	○○	+
Layer V		•	○○	+
Layer VI		•	○○	+
White matter (interstitial cells)			○	
Hippocampal formation				
Fascia Dentata	- Str. Moleculare, outer 2/3	●●		++
	inner 1/3	●	○	+
	- Str. Granulare		○○	+
	- Hilus	•	○○	+
Ammon's horn	- Str. Lacunosum-moleculare	●●		++
	- Str. Radiatum	●	○	+
	- Str. Pyramidale		○○	+
	- Str. Oriens	•	○	+
	- Alveus			
Subicular complex	- Str. Moleculare	●●		++
	- Str. Pyramidale	•	○○	+
	- Str. Oriens	●	○	+
Entorhinal cortex				
Layer I		●●		++
Layer II		●	○○	+
Layer III		•	○○	+
Layer IV		•	○○	+
Layer V		•	○○	+
White matter (interstitial cells)		●		+
Olfactory areas				
Prepyriform cortex	- Molecular layer	●●	○○	++
	- Pyramidal layer	●	○○	+
	- Polymorph layer	•	○○	+
Lateral olfactory tract				++
N. of the lateral olfactory tract		•	○○	++
Corticomedial amygdaloid nuclei		●●	○○	+
Other telencephalic structures				
Basolateral amygdaloid nuclei		•	○○	+
Central amygdaloid nucleus		•	○○	+
Intercalated cell masses of amygdala		•	○○	+
Stria terminalis		•		+
Bed nucleus of stria terminalis		•	○○	+
Substantia innominata		●●	○	+
Claustrum		•	○○	+
Striatum **			○○	+
Globus pallidus (L+M)			○○	+
Diencephalon				
Hypothalamus	- Paraventricular N.	●●	○	+
	- Periventricular N.	•	○○	+
	- Other nuclei.		○○	+
Reticular nucleus			○○	+
Zona incerta / Fields of Forel		•	○○	+
Thalamic nuclei ***			○○	+
Habenular nuclei			○○	+
Pretectal nuclei ****		●	○○	+
Brainstem				
Superior colliculus			○○	+
Periaqueductal gray			○○	+
Substantia nigra			○	+
Raphe nuclei			○○	+
Pontine nuclei			○○	+
Superior olivary nuclei			○○	+
Parabrachial nuclei			○○	+
Cochlear nuclei			○○	+
Vestibular nuclei			○○	+
Trigeminal complex			○○	+
Brainstem motor nuclei *****			○○	+
Reticular nuclei			○○	
Cerebellum				
Molecular layer			○	++
Purkinje cell layer			○○	+
Granular layer			○○	+
Cerebellar white matter				
Deep cerebellar nuclei			○○	+

For descriptive purposes, labeled neuronal somata are classified in two main categories: those containing solid immunoprecipitate (SReln-ir neurons, black circles) and those displaying discrete immunoreactive particles (PReln-ir neurons, open circles). Circles represent a gross approximation of the relative number of each type of immunoreactive somata in a nucleus or layer (one small circle: occasional isolated cells; one large circle: numerous cells; two large circles: all, or the great majority of neurons are labeled). Likewise, crosses are used to represent differences in the density of neuropil immunoreactivity (+: sparse labeling; ++: dense labeling). Note that virtually all the examined brain regions contained immunoreactive somata and neuropil. The only exceptions were the cerebral white matter, which contained a few occasional labeled interstitial neurons, and the cerebellar white matter, which did not contain any labeling.

*Cortical areas examined: prefrontal (dorsolateral, medial, orbitofrontal), premotor, motor, somatic sensory, posterior parietal, temporal (association, auditory, perirhinal), insular, cingulate, retrosplenial and occipital (striate and peristriate).

**Striatal nuclei examined: caudate (head, body and tail), putamen and accumbens.

***Thalamic nuclei examined: paratenial, reuniens, centromedian, ventral posterior, mediodorsal, pulvinar complex, lateral and medial geniculate complexes.

****Somata with solid immunolabeling were only observed in the nucleus of the posterior commissure.

*****Brainstem motor nuclei examined: oculomotor, trigeminal motor, abducens and facial nuclei.

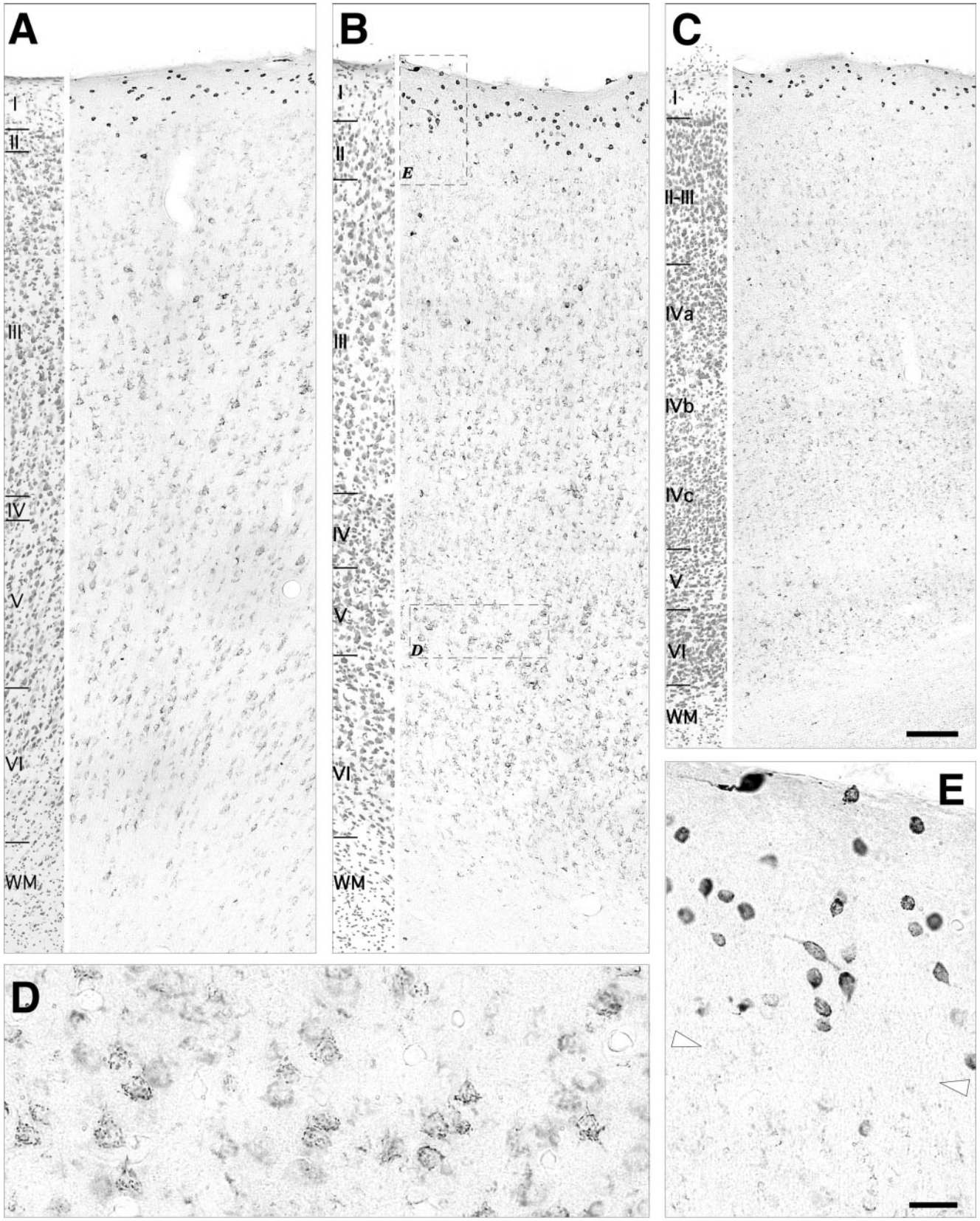

Figure 1. Reelin immunoreactivity in the macaque isocortex. Diaminobenzidine staining without metal enhancement. (*A–C*) Low-magnification coronal samples taken from three separate cortical areas: dorsal premotor cortex (*A*), posterior cingulate cortex (*B*), and primary visual cortex (*C*). Pial surface is at the top. In each sample, a narrow stripe from an adjacent, Nissl-stained section is shown to provide an approximate reference for the density of cells in each layer (I–VI). Note that the Nissl stain includes glial and endothelial cells. WM = subcortical white matter. Bar = 100 μm. (*D*) Labeling in layer V of the posterior cingulate cortex (inset in *B*). Note that virtually all the pyramidal neurons display small immunoreactive particles in their somata. (*E*) Labeling in the superficial layers of the posterior cingulate cortex (inset in *B*). Neurons with continuous labeling of their somata and proximal dendrites populate layer I, while light particulate labeling is present only in the layer II neurons. This abrupt change traces the layer I/II border (arrowheads).

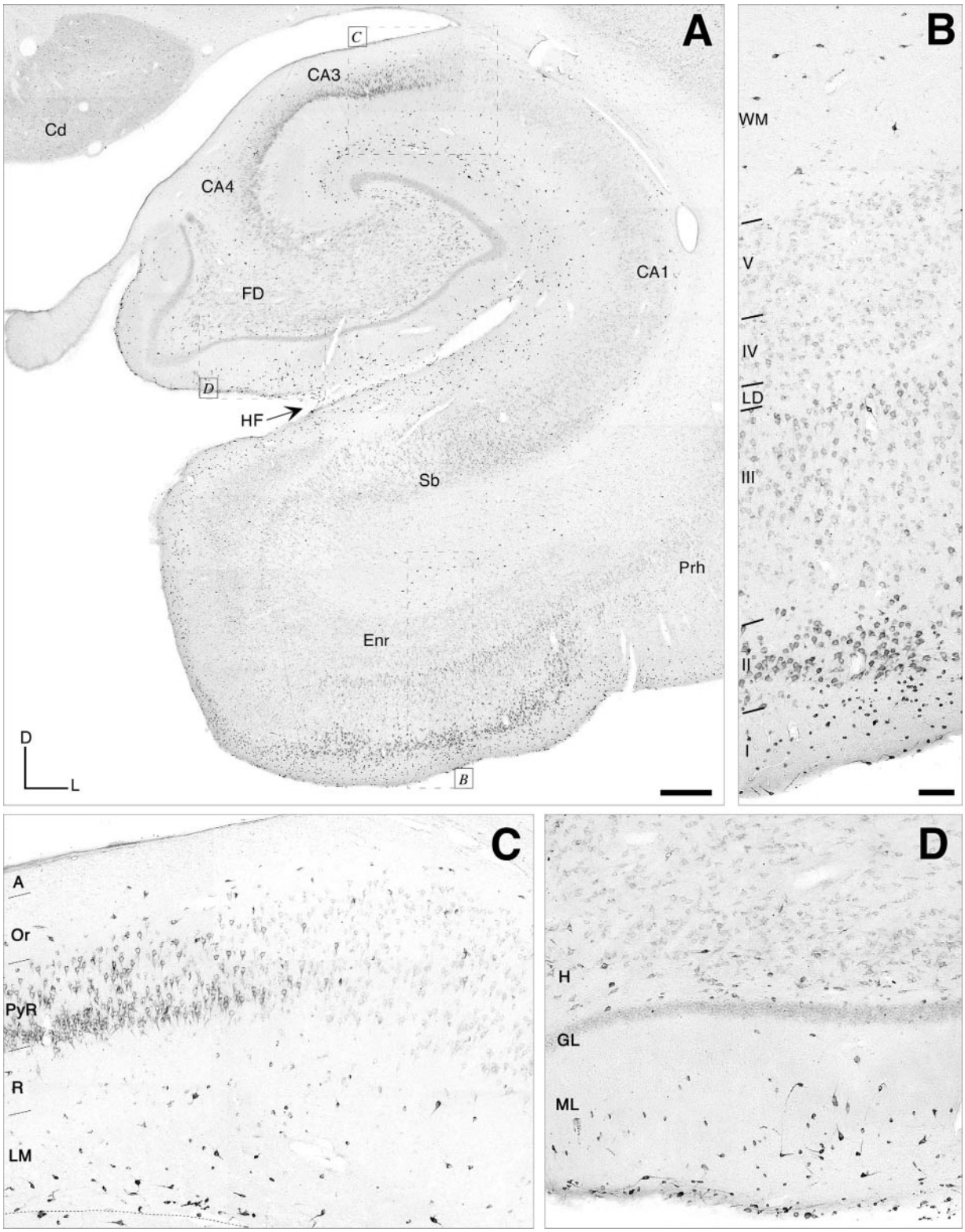

Figure 2. Reelin immunoreactivity in the hippocampal formation and parahippocampal cortex. Diaminobenzidine staining without metal intensification. (*A*) Panoramic view of a coronal section across the body of the hippocampus. The tail of the caudate nucleus (Cd, upper right corner) is also shown. Most neuronal somata in all fields are immunoreactive; however there are striking differences in the labeling pattern between the various fields and layers. Notice, for example, the difference between the Ammon's horn sectors 3 (CA3) and 1 (CA1), or between the entorhinal (Enr) and perirhinal (Prh) areas. FD: fascia dentata; HF: hippocampal fissure; Sb: subiculum. (*B*) Detail of the labeling in the entorhinal cortex (inset in *A*). Superficial (I, II, III) and deep cellular layers (IV–V); lamina dissecans (LD). The labeling pattern of neuronal bodies is markedly lamina specific. Notice also the heavily immunoreactive interstitial neurons of the subcortical white matter (WM, top). (*C*) Transitional region between the CA3 and CA1 fields (inset in *A*). Stratum lacunosum–moleculare (LM), stratum radiatum (R), stratum pyramidale (PyR), stratum oriens (Or) and alveus (A). Note that while labeling in the pyramidal stratum shifts abruptly, the labeling pattern in other layers is similar in the two fields. (*D*) Fascia dentata (FD, inset in *A*). Molecular layer (ML), granule cell layer (GL) and hilum (H). In this panel (and in *C* – LM and *D* – layer I), notice the population of medium-sized (15–20 μm) neurons in ML that display solid labeling of their soma and one or two long dendrites. These long dendrites form an immunoreactive subpial plexus best appreciated in *D*.

neurons. However, at high magnification, it was evident that most of the particles in PReln-ir cells were heavily labeled, although they were too small to be seen at low magnification under bright-field optics. These particles were sharply delineated corpuscles of widely varied shapes, ranging from lump-like to fiber-like. Fiber-like particles were very thin (0.1–0.5 μm), elongated (up to 100 μm), and often varicose, tortuous or branched. Lump-like particles varied from small pellets (0.1–0.2 μm) to larger irregular masses of several microns in diameter. Overall, the varied morphology and arrangement of these particles in the labeled cells conferred an appearance that was specific to the neurons in each nucleus or layer, or even to particular cell types (Fig. 3*A*1–*I*4).

In non-counterstained tissue sections, large aggregates of immunoreactive particles clearly delineated the soma of some PReln-ir neurons, but isolated particles were often difficult to relate to a cell soma (Fig. 1*D*,*E*). In cresyl-violet counterstained sections (Fig. 3), however, it was readily evident that the immunoreactive particles always co-localized with neuronal somata. Those of filiform shape were mainly found in the dendritic shafts of neurons, while lump or pellet-like particles were located around the neuronal nuclei. What was more, counterstaining confirmed that the nuclei and large parts of the cytoplasm of the PReln-ir neurons were unlabeled.

In the SReln-ir neurons, the immunolabeling covered the whole soma and proximal dendrites, but spared the nucleus. Although the labeling extended up to second-order branches in the dendrites of some of these cells, in most it was limited to dendritic shafts. Interestingly, the labeling in SReln-ir neurons showed spots of higher density, in a manner reminiscent of the particles observed in PReln-ir cells (Figs 1*E*, 3*A*1–2, 3*B*2, 3*G*5).

Cresyl violet counterstaining revealed that some cell populations were not immunoreactive for Reelin. The vast majority of these cells were identified either as glial cells, due to their small (<2 μm), heavily stained nucleus, or as endothelial cells, due to their elongated nucleus and perivascular position (Fig. 3*A*1–4). However, in many brain regions, some non-immunoreactive cells were clearly neurons (Fig. 3*A*1–2, 3*B*3–4, 3*C*). In most cases their size was in the range of the smaller neurons in the corresponding nucleus or layer. Although we cannot generalize across so many brain regions, these observations suggest that, in most cases, the Reelin-immunonegative neurons were interneurons.

Axonal and Neuropil Immunoreactivity

The axons of the lateral olfactory tract and of the stria terminalis showed a peculiar type of immunolabeling (Fig. 4). These axons displayed very small (<0.2 μm), apparently intraaxonal immunoreactive puncta, while the rest of the axon was unlabeled (Fig. 4*B*,*D*). In addition, heavy neuropil labeling consisting of the same type of immunoreactive particles was present in the external division of the anterior olfactory nucleus (Fig. 4*B*), a terminal field of the lateral tract axons (Carmichael *et al.*, 1994). We did not systematically examine other terminal fields of the tract, but this observation does suggest that Reelin is transported along the axons from the olfactory bulb, and probably also along those of the stria terminalis. We did not observe similar immunoreactivity in most of the other white matter tracts (Table 1, Fig. 4*A*).

The gray matter neuropil of most brain areas contained large numbers of immunoreactive puncta, so small that they were evident only at high magnification (Fig. 3*A*1–3, 3*B*1–2, 3*B*4–*I*2). Al low magnification, these puncta appeared as a faint background staining, that was particularly dense near the pial surface of the cerebral and cerebellar cortices. When examined through the depth of focus in a section, the immunoreactive puncta often displayed loose linear arrangements, like beads strung on a thread. The absence of similar labeling in the cerebral and cerebellar white matter, or in control tissue sections in which the primary antibody had been omitted, indicated that this labeling was Reelin specific.

Reelin Immunoreactivity in the Isocortical Areas of the Cerebral Cortex

We examined most isocortical fields, including sensory, association, limbic and motor areas. The labeling pattern was fairly similar throughout the isocortex. The slight fluctuations between areas basically reflected the underlying cytoarchitectonic differences. Samples from three areas are illustrated in Figure 1.

Most neurons in isocortical layers II–VI were PReln-ir. The large pyramidal cells in layers III and V showed conspicuous aggregates of immunoreactive particles, but even the small pyramidal, stellate and fusiform cells in layers II–VI contained some thin particles. Filiform particles extended along the shaft of dendrites, while lump-like particles surrounded the cell nucleus, particularly near the base of the dendrites (Fig. 3*A*2–4).

A conspicuous population of SReln-ir neurons was present in layer I; in fact, all the neurons labeled in this layer were SReln-ir, even if with different intensities of staining (Fig. 1*E*). Most of these cells had small (5–8 μm) round or fusiform bodies, and bitufted or multipolar dendritic arrangements. In addition, relatively large neurons (10–20 μm soma size) with one or two thick, long and poorly branched dendrites extending parallel to the cortical surface were occasionally observed immediately beneath the pia. The somata of these cells were so superficial that they often bulged on the cortical surface (Fig. 3*A*1). These large subpial neurons were observed in the medial limbic areas more often than in frontopolar, occipital or dorsolateral isocortical areas (Fig. 1*A*–*C*). An additional, smaller population of SReln-ir neurons was scattered throughout layers II–VI, but mostly in II–III. These cells resembled the small SReln-ir neurons of layer I. A few interstitial cells in the white matter were SReln-ir (Table 1).

Nissl counterstaining showed a relatively small population of isocortical neurons in all layers that was not immunoreactive for Reelin (Fig. 3*A*1–2). The soma size of these neurons was similar to that of the smallest isocortical neurons (~5 μm). Neuropil labeling was present in all cortical layers, and densest near the pial surface in layer I (Fig. 3*A*1–4).

Reelin Immunoreactivity in the Hippocampal Formation and Entorhinal Cortex

Temporomedial cortical areas contained large numbers of immunoreactive neuronal somata (Fig. 2). The pyramidal neurons in Ammon's horn (CA), subiculum and entorhinal cortex were PReln-ir. Moreover, virtually all of the fascia dentata (FD) granule cells were PReln-ir as well. This labeling varied markedly between adjacent fields or layers. This was evident, for example, at the border between the entorhinal and perirhinal cortices (Fig. 2*A*); between CA sectors 3 and 1 (Figs 2*C*, 3*B*4, 3*B*5); or between the layers of the entorhinal cortex (Fig. 2*B*). Interestingly, in the case of the CA pyramids, the difference in staining intensity was due to a heavier staining of similarly sized particles, rather than an increase in the number of labeled particles (compare Fig. 3*B*4 and 3*B*5).

The subpial layer of hippocampal formation areas (layer I of the entorhinal cortex, stratum lacunosum–moleculare of the subiculum and CA, or stratum moleculare of FD) contained

numerous heavily stained SReln-ir neurons. The morphology of these cells resembled that of SReln-ir cells in isocortical layer I; however, larger neurons (10–20 μm), with tangential dendritic arrangements, were more abundant here, while smaller SReln-ir neurons were relatively scarcer, particularly in CA and FD (Fig. 2). The large SReln-ir neurons were preferentially situated near the pial surface of the hippocampal fissure. The oriens and radiatum strata of CA contained additional populations of SReln-ir neurons (Fig. 3*B*3). The somata (5–15 μm) of these neurons were predominantly fusiform or multipolar. Their morphology and laminar location suggests that they were mainly interneurons; however, it is also possible that at least some cells in the stratum oriens corresponded to non-pyramidal neurons projecting to the septum (Rosene and Van Hoesen, 1987). Similar SReln-ir neurons were observed in the hilar region of FD (Figs 2*A*, 2*D*, 3*B*3), as well as in the white matter of the entorhinal cortex (Fig. 2*B*).

Nissl counterstaining revealed several interneuron populations in the hippocampal formation that were not immunoreactive for Reelin. These included neurons in the hilus and the molecular stratum of FD, and the strata radiatum and oriens of CA (Fig. 3*B*3–4).

Neuropil labeling was present in all layers of FD, CA (except in the alveus), subiculum and entorhinal cortex, and it became particularly heavy in the superficial third of the molecular layer of FD and stratum lacunosum–moleculare of CA (Fig. 3*B*1–2).

Reelin Immunoreactivity in Subcortical Structures

Most subcortical regions displayed large numbers of PReln-ir neuronal somata (Table 1, Fig. 3*C*–*I*4). In the striatum, most neurons contained small and weakly immunoreactive particles. A population of slightly larger, striatal cells containing larger and more intensely immunoreactive particles was present all over the caudate (Fig. 2*A*) and putamen (Fig. 3*E*). Virtually all the neurons in the globus pallidus were PReln-ir (Fig. 3*F*). All nuclei in the thalamus, including the reticular nucleus, contained a majority of PReln-ir neurons. Labeling was similar in most thalamic nuclei (Fig. 3*G*1–2), except for the magnocellular layers of the dorsal lateral geniculate (Fig. 3*G*3–4) and the nucleus reuniens, which were fairly more heavily labeled. Most other diencephalic nuclei and virtually all brainstem nuclei also contained a large majority of PReln-ir neurons (Table 1). Particularly notable are the large particles that appear to wrap around the cell nucleus in the neurons of the dorsal (Fig. 3*G*5, top) and suprachiasmatic nuclei of the hypothalamus; the clustering of round particles in the soma and long filiform particles in the dendrites in the brainstem motoneurons (Fig. 3*H*2); and the complex ramified particles of the superior olivary nuclei (Fig. 3*H*3). The neurons in the pontine (Fig. 3*I*3) and deep cerebellar nuclei were heavily PReln-ir. In the cerebellar cortex, virtually all the granule cells were PReln-ir; in addition, other larger neurons in the granular layer, presumably Golgi cells, showed similar labeling (Fig. 3*I*4). The molecular layer contained scattered PReln-ir neurons, presumably stellate and/or basket cells (Fig. 3*I*1). Strikingly, all the Purkinje cells were conspicuously PReln-ir (Fig. 3*I*2).

Basal telencephalic regions (Table 1), particularly those nuclei located near the pial surface (medial septal nucleus, diagonal band, cortical and medial amygdaloid nuclei), contained numerous SReln-ir neurons (Fig. 3*C*). In the diencephalon, SReln-ir neurons were only observed in two regions: the paraventricular–periventricular nucleus of the hypothalamus (Fig. 3*G*5), and the nucleus of the posterior commissure (not illustrated). Remarkably, the brainstem and cerebellum contained no SReln-ir cells.

Most subcortical gray matter structures displayed neuropil immunoreactivity (Table 1). Labeling was particularly heavy in the molecular layer of the cerebellum (Fig. 3*I*1).

Subcellular Localization of the Reelin Immunostaining

The morphology of the labeling in neuronal somata and proximal dendrites in Nissl-counterstained 50 μm thick sections strongly suggested that the immunolabeling was located intracellularly. Examination of semithin (2–3 μm thick) immunoreacted sections counterstained with toluidine blue showed that, in fact, Reelin immunoreactivity was always located within the neuronal cytoplasm. In the PReln-ir neurons, the immunoreactive particles surrounded the nucleus and often extended along the stalk of the main dendrites, leaving the rest of the cytoplasm unstained (Fig. 3*J*,*L*). In the SReln-ir neurons, the labeling extended irregularly but covered the whole cytoplasm of their neuronal somata. Since these cells were mainly interneurons, their cytoplasmic area was relatively small; nevertheless, spots of heavy immunolabeling alongside weakly stained regions were apparent within it (Fig. 3*K*). Neither PReln-ir nor SReln-ir cell nuclei showed immunolabeling.

The light microscopy appearance of the immunoreactive particles was strongly suggestive of Reelin epitope association with specific cell organelles, particularly with the endoplasmic reticulum and Golgi complex (De Camilli *et al*., 1986; Gonatas, 1994). To confirm this possibility, we prepared thin (60–80 nm) sections of neurons identified as either PReln-ir or SReln-ir in semithin sections, and examined them with a transmission

Figure 3. Fine morphology and intracellular localization of Reelin immunolabeling in cortical and subcortical neurons. (*A*1–*I*4) High-magnification samples taken from different brain regions. Nickel-enhanced diaminobenzidine immunostaining with cresyl violet counterstain. Bar for *A*1–*I*4 (shown in panel *H*3) = 25 μm. (*A*1) Superficial half of layer I, posterior parietal cortex. Pial surface is at the top. (*A*2) Layer I–layer II border, posterior parietal cortex. (*A*3) Layer III, posterior parietal cortex. (*A*4) Layer V, posterior parietal cortex. (*B*1) Superficial third of the molecular layer, fascia dentata. (*B*2) Stratum lacunosum–moleculare, Ammon's horn sector 1. (*B*3) Granule cell layer (top) and hilum (bottom) of fascia dentata. (*B*4) Pyramidal layer, Ammon's horn sector 3. (*B*5) Pyramidal layer, Ammon's horn sector 1. (*C*) Basal amygdaloid nucleus. (*D*) Layer II, entorhinal cortex. (*E*) Putamen. (*F*) Lateral globus pallidus. (*G*1) Pulvinar thalamic complex. (*G*2) Reticular thalamic nucleus. (*G*3) Parvocellular layers, dorsal lateral geniculate thalamic nucleus. (*G*4) Magnocellular layers, dorsal lateral geniculate thalamic nucleus. (*G*5) Paraventricular hypothalamic nucleus. (*G*6) Parataenial thalamic nucleus. (*H*1) Mesencephalic nucleus, trigeminal nuclear complex. (*H*2) Motor nucleus, trigeminal nuclear complex. (*H*3) Lateral nucleus, superior olivary complex. (*H*4) Substantia nigra, pars compacta. (*H*5) Centralis superior raphe nucleus. (*H*6) Pontine nuclei. (*H*7) Parabrachial nuclei. (*H*8) Dorsal cochlear nucleus. (*I*1) Molecular layer, cerebellar cortex. (*I*2) Purkinje cell layer, cerebellar cortex. (*I*3) Dentate cerebellar nucleus. (*I*4) Granule cell layer, cerebellar cortex. Nissl counterstain reveals that the immunoreactive particles overlap neuronal somata and proximal dendrites. These intracellular particles appear to surround the cell nucleus, and display a remarkably different shape and caliber depending on the region and cell type. Nissl counterstaining also shows that some cells are not immunoreactive for Reelin; most of these have small (2–3 μm) darkly stained nuclei and are thus presumably glial cells, but some are larger and paler, and are presumably neurons (arrows in *A*1, *A*2, *B*3, *B*4 and *C*). In addition to immunoreactive neuronal somata, note that, in many structures, a finely grained immunoprecipitate is evident in the neuropil (*A*1, *A*3, *B*1, *B*2, *B*5, *G*2, *G*6 and *I*1). (*J*–*L*) Semithin sections of immunoreacted tissue with toluidine blue counterstaining. Bar for *J*–*L* = 5 μm. (*J*) A layer III pyramidal cell from the rostral prefrontal cortex. Pial surface is at the top. Note the elongated immunoreactive particles in the cytoplasm around the nucleus and in the stem of the apical dendrite. (*K*) A layer II multipolar interneuron of layer II in the rostral prefrontal cortex with solid Reelin immunostaining (SReln-ir). The labeling covers the whole cytoplasm of the cell soma. (*L*) A cerebellar cortex Purkinje cell. Nickel-enhanced DAB immunostaining. Note, as in *J*, that the large immunoreactive particles surrounding the nucleus are clearly separated from the plasmalemma.

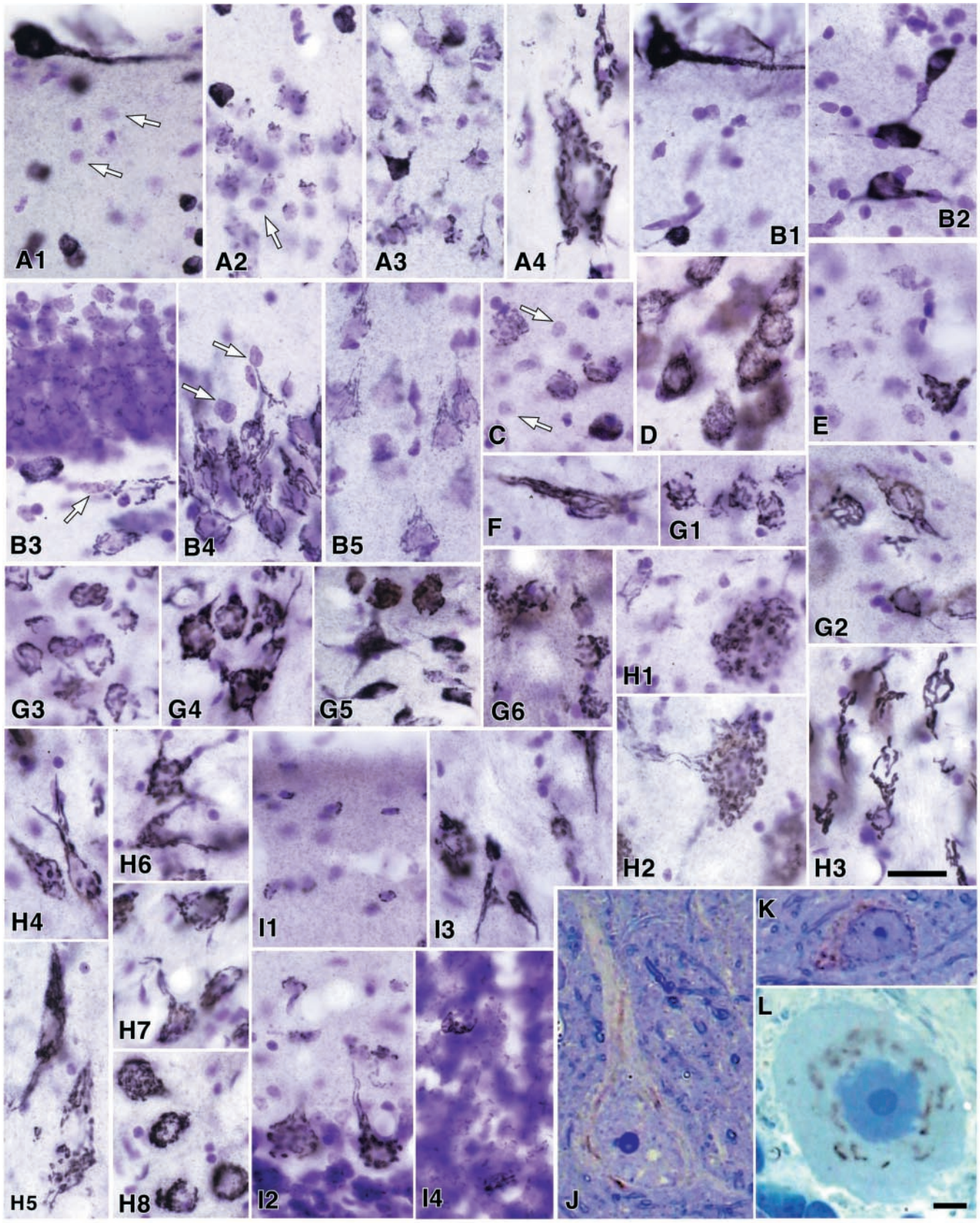
A1
A2
A3
A4
B1
B2
B3
B4
B5
C
D
E
F
G1
G2
G3
G4
G5
G6
H1
H2
H3
H4
H5
H6
H7
H8
I1
I2
I3
I4
J
K
L

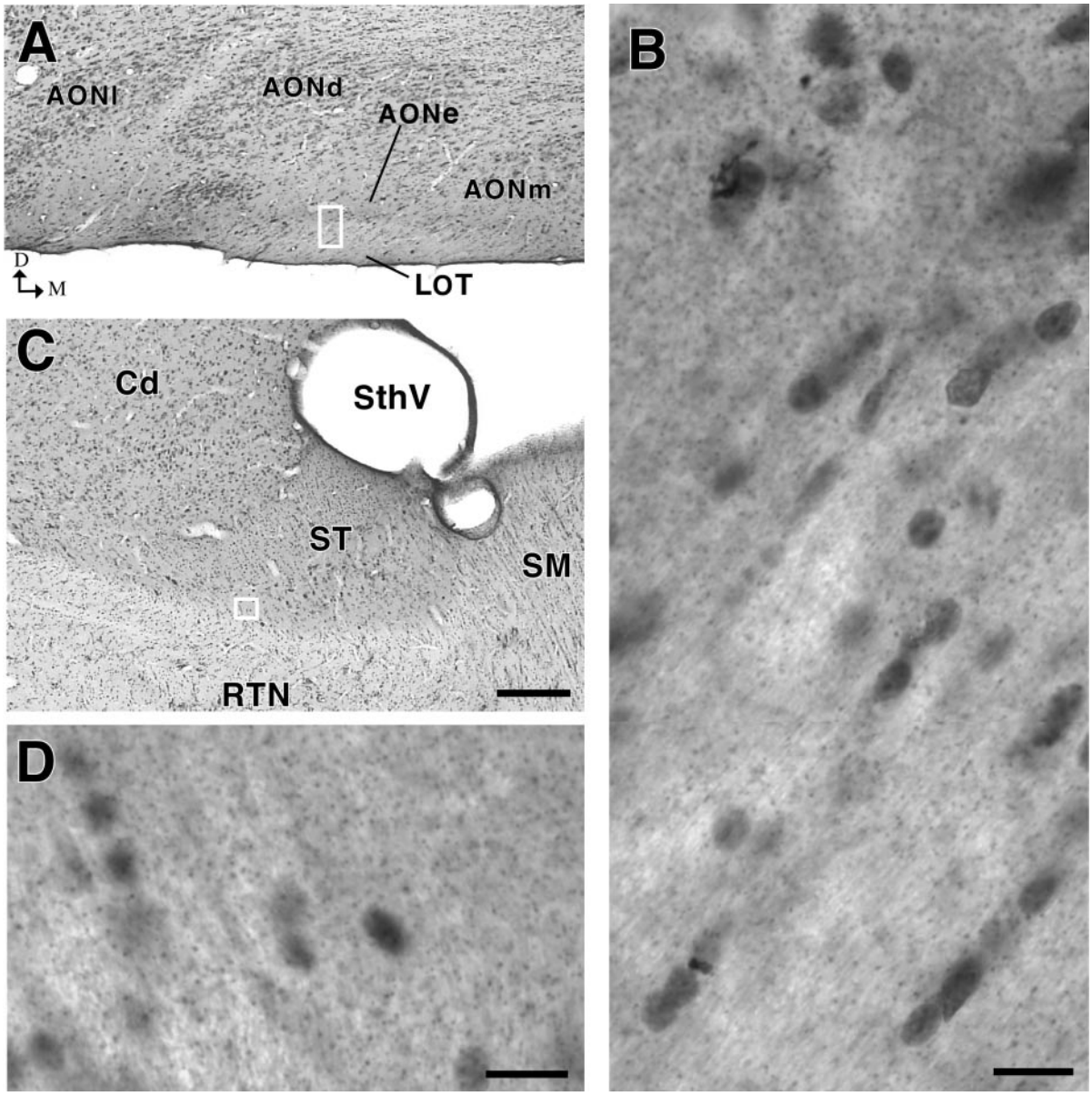

Figure 4. Reelin may be transported over long distances along some axonal pathways. Nickel-enhanced DAB immunostaining. For cytoarchitectonic identification, the sections are counterstained with cresyl violet; visible cell somata thus mainly correspond to cresyl violet stained cells. (*A*, *B*) Labeling in the anterior olfactory nuclear complex in the orbital surface of the frontal lobe. The lateral olfactory tract (LOT) is visible at the pial surface in *A*. The high magnification image in *B* (inset in *A*) illustrates the heavy punctate immunostaining in the LOT axons and their terminal arborizations. The lower two-thirds of the image in *B*, which correspond to the axonal trunks of the lateral olfactory tract, shows labeled puncta arranged in rows parallel to the direction of the axons, while in the upper part of the image, which corresponds to a terminal field of the axons in the external division of the anterior olfactory nucleus [AONe (Carmichael *et al*., 1994)], the labeled puncta are randomly distributed. (*C*, *D*) Labeled axons in the stria terminalis (ST). The image in *D* (inset in *C*), shows large numbers of immunoreactive puncta in the ST axons. Note in *D* that the labeled puncta are aligned in rows parallel to the direction of the fibers. At low magnification (panel *C*) the axonal labeling darkens the ST in comparison to other adjacent white matter tracts such as the stria medularis (SM) or the white matter surrounding the reticular thalamic nucleus (RTN). Other abbreviations: AONl = lateral division of the anterior olfactory nucleus; AONd = dorsal division of the anterior olfactory nucleus; AONm = medial division of the anterior olfactory nucleus. Cd = body of the caudate nucleus; SthV = striatothalamic vein. Bar in *A* and *C* = 500 μm; in *B* and *D* = 5 μm.

electron microscope. Some of the resulting images are presented in Figure 5.

The overall immunoreactivity in the glutaraldehyde-fixed tissue used for electron microscopy was lower than in the sections fixed only with paraformaldehyde analyzed with light microscopy. Immunostained complexes of elongated membranous cisternae were recognizable in the cytoplasm of the SReln-ir and PReln-ir neurons around the nuclear membrane. Labeling was heavier and more continuous in the cisternae of the SReln-ir cells (Fig. 5*B–C*) than in those of the PReln-ir cells (Fig. 5*F–H*,*K*). Labeled cisternae in SReln-ir cells included both closely apposed (~30 nm of separation between adjacent cisternae) and more separated (~150 nm) cisternae (Fig. 5*B–C*). These features indicate (Peters *et al*., 1991) that the labeling in SReln-ir cells involved the endoplasmic reticulum and the Golgi complex. In the PReln-ir cells, the labeled cisternae exhibited the typical morphology of the Golgi complex. These cisternae were either located around but at some distance from the nuclear membrane, or along the dendritic shafts (Fig. 5*D–E*,*I–J*). The SReln-ir neurons, but not the PReln-ir neurons contained, in addition to these labeled membranous organelles, an amorphous immunoprecipitate throughout the cytoplasm (Fig. 5*A–B*).

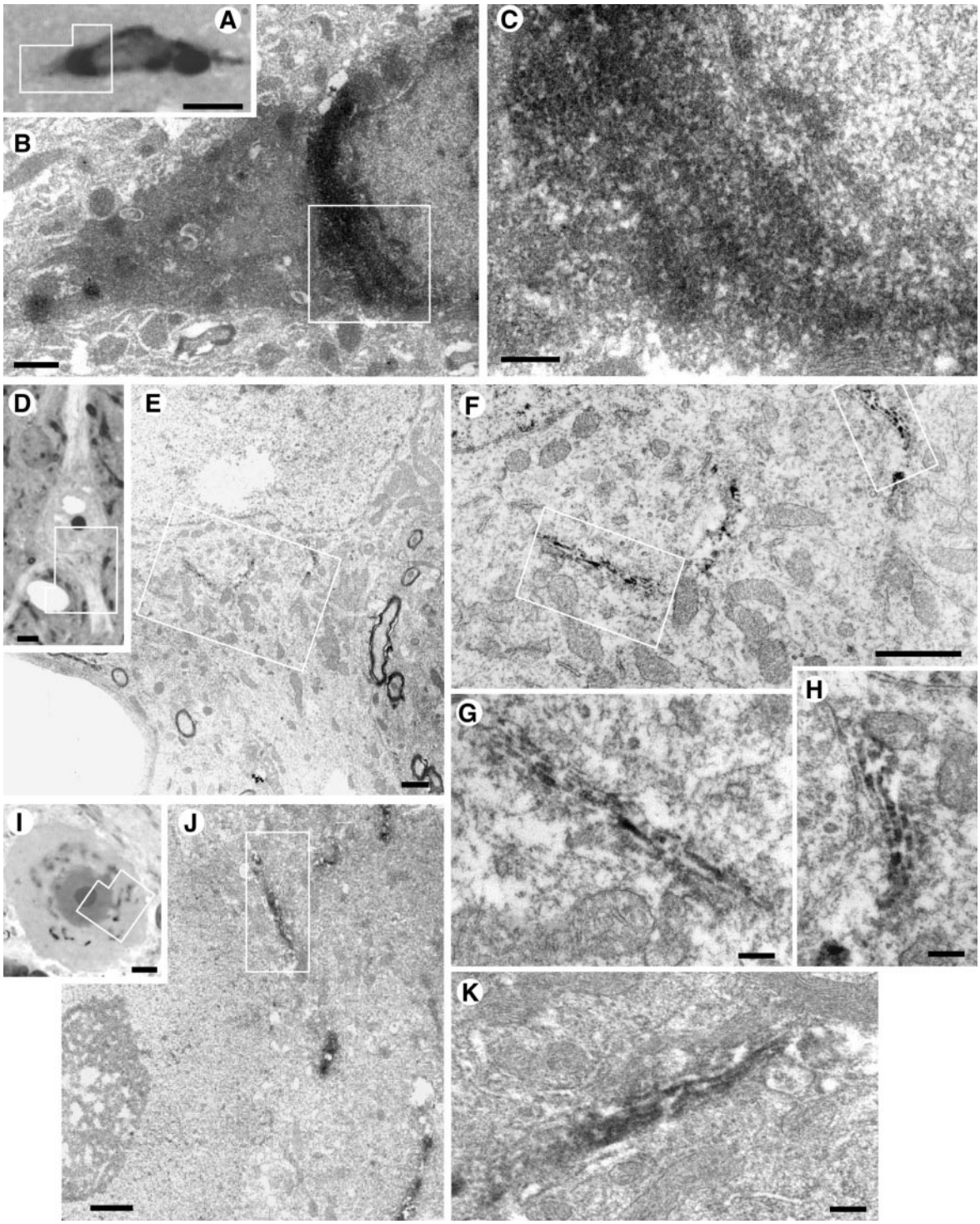

Figure 5. Subcellular localization of Reelin immunoreactivity in cortical and cerebellar neurons. (*A–C*) A horizontal interneuron of the stratum lacunosum–moleculare of the hippocampus with long tangential dendrites (compare with Figs 2*C* or 3*B*2) that displays solid Reelin immunostaining (SReln-ir). (*A*) Photomicrograph of a semithin section with Nickel-enhanced DAB immunostaining and toluidine blue counterstain. (*B*) Electron micrograph of an ultrathin section taken from the same cell (inset in *A*). Note the large, heavily stained system of cisternae nested as a cap near the nuclear membrane, at the base of a dendrite, as well as the weaker, diffuse staining throughout the cell cytoplasm. (*C*) Detail of the heavily immunoreactive cisternae (inset in *B*). The morphology and distance between the cisternae (~150 nm), as well as their perinuclear location and parallel orientation to the nuclear membrane suggest that they are part of the endoplasmic reticulum. (*D–H*) A pyramidal cell in layer V of the rostral prefrontal cortex that displays particulated Reelin immunolabeling (PReln-ir compare with Figs 1*D* or 3*A*4). (*D*) Photomicrograph of a semithin section with toluidine blue counterstaining. Three thin elongated structures are visible at the base of a basal dendrite. (*E*) Electron micrograph of the cell illustrated in *D* (inset). Note that the same three immunoreactive structures are recognizable. They are oriented towards the dendrite, and mainly perpendicular to the nuclear membrane. Bar = 2 μm. At higher magnification (*F–H*) it is evident that the immunoreactive structures are membrane cisterns whose morphology and close (~30–50 nm) parallel stacking demonstrate that they are part of the Golgi complex. Images *G* and *H* correspond to the insets in *F*. (*I–K*) A Purkinje cell of the cerebellar cortex. (*I*) Photomicrograph of a semithin section. Nickel-enhanced DAB immunostaining with toluidine blue counterstaining. Note the numerous large immunoreactive structures in the cell cytoplasm. (*J*) Electron micrograph of the inset in *I*. Several immunoreactive structures are visible at different distances from the nuclear membrane. (*K*) A high-magnification view of the immunoreactive particles (inset in *J*) shows that the labeling is associated with a system of Golgi cisterns. Calibration bar for *A* = 2 μm; *C* = 200 nm; *D*, *I* = 5 μm; *F* = 500 nm; *G*, *H*, *K* = 200 nm; *J* = 1 μm.

Discussion

Overview of results

We have systematically mapped both the immunoreactivity to Reelin protein in cortical and subcortical regions of the adult macaque brain, as well as the subcellular localization of the immunoprecipitate in cells of the cerebral cortex and cerebellum. Our results show that a great majority of adult macaque brain neurons, including projection neurons and interneurons, are immunoreactive for Reelin. Although the immunolabeled neuronal somata show a wide spectrum of staining patterns, most could be readily ascribed to either one of two basic categories: (a) labeling of discrete intracytoplasmic particles with widely varying shapes and sizes (PReln-ir cells), or (b) solid staining of the cytoplasm and proximal dendrites (SReln-ir cells). In addition to their adequacy for descriptive purposes, these different patterns might reflect substantial differences in protein expression levels, and/or in protein trafficking.

The PReln-ir neurons were far more numerous, and were found in all brain, cerebellar and brainstem regions, whereas the SReln-ir cells were largely restricted to cortical telencephalic structures. In addition, several brain regions, including the cerebral cortex, contained relatively small interneuron populations that were not immunoreactive for Reelin. Electron microscopy data indicate that in PReln-ir neuronal somata, the labeling is associated with the Golgi complex, whereas in the SReln-ir cells, as well as in the Golgi complex, it is also present in the endoplasmic reticulum and cytoplasm.

In addition to neuronal somata, the neuropil of all cortical and subcortical gray matter regions displays finely grained immunostaining. In our material, it is unclear whether this labeling corresponds to axons, dendrites, or both. However, the observation that some long fiber tracts showed a punctate immunolabeling along their axons and terminal fields (Fig. 4), indicates that, in some projection neurons, Reelin could be transported in tiny particulate structures along the axons to the terminal arborizations. These observations concur with recent electron microscope observations in embryonic mice Cajal–Retzius cells to the effect that Reelin is contained in discrete, and would be secreted from, membrane-bound vesicles within the axons of these cells (Derer *et al.*, 2001). Similarly, the heavy immunolabeling in the neuropil of the molecular layer of the cerebellum has been attributed to Reelin transport along granule cells axons (Pesold *et al.*, 1998). The fact that Reelin can be transported over long distances through some axonal systems may be relevant in accounting for the localization of Reelin protein in the neuropil of at least some brain regions. Nevertheless, it is as yet unclear whether this is a general mechanism, since, apart from the lateral olfactory tract and the stria terminalis, we could not detect unambiguous Reelin immunoreactivity in other white matter tracts.

Below, we compare our results with available reports of Reelin mRNA or protein distribution in the adult brain of other species, and then explore some of the implications that the observed pattern of Reelin distribution may have for our understanding of the functional roles of this protein in the adult primate brain.

Most Projection and Local Circuit Neurons in the Cerebral Cortex Contain Reelin

Our observations regarding SReln-ir neurons in the cerebral cortex confirm and extend previous observations in adult primates (Rodríguez *et al.*, 2000; Zecevic and Rakic, 2001), including humans (Impagnatiello *et al.*, 1998; Fatemi *et al.*, 2000; Guidotti *et al.*, 2000), that several interneuron populations, mainly in cortical layer I, but also in deeper layers, are strongly immunoreactive for Reelin. Several similar populations of Reelin-positive cortical interneurons have also been found in adult rodents and carnivores (Pesold *et al.*, 1998, 1999; Pérez-García *et al.*, 2001; Martínez-Cerdeño and Clascá, 2002).

The relatively large (~20 μm) SReln-ir subpial interneurons with thick and largely tangential dendrites observed in our macaques are more frequently found in medial limbic isocortical areas, entorhinal cortex and hippocampal formation than in dorsolateral, frontal and occipital isocortical areas, while the smaller layer I interneurons appear in roughly equivalent numbers. The large subpial Reelin-immunoreactive cells have been considered a remnant of the Cajal–Retzius cell population generated in embryonic life (Meyer and Goffinet, 1998; Zecevic and Rakic, 2001). It is thus tempting to speculate that their uneven distribution might, in part, reflect a more marked 'dilution effect' in the cortical areas that undergo pronounced growth in the later developmental stages of primates (Blinkov and Glezer, 1968; Marin-Padilla, 1998). Interestingly, we observed a substantial population of large tangential (Cajal–Retzius like) interneurons in the adult macaque hippocampus (Fig. 2), while studies in mice hippocampus have reported that similar, tangentially oriented 'Cajal–Retzius' cells die postnatally (Del Rio *et al.*, 1995, 1996).

We show here that virtually all the pyramidal neurons in the monkey isocortex, mesocortex and archicortex contain significant amounts of intracellular Reelin in their soma, and that a large fraction of the protein is located within the Golgi apparatus. In contrast, Reelin-containing pyramidal cells appear to be much less numerous in rodents and carnivores, where only some layer V pyramidal cells, and the layer II pyramidal cells of the entorhinal cortex, are immunoreactive for Reelin (Pesold *et al.*, 1998; Pérez-García *et al.*, 2001; Martínez-Cerdeño and Clascá, 2002). Similarly, the FD granular cells are heavily PReln-ir in macaques (present results), but not in rodents (Pesold *et al.*, 1998) or carnivores (V. Martínez-Cerdeño and F. Clascá, unpublished observations).

In humans, immunoreactive pyramidal cells with a particulate staining have been reported in layers II and III of the entorhinal cortex (Pérez-García *et al.*, 2001), but not in the isocortical areas. The significance of these findings in humans is unclear, given the fact that the immunostained brain samples were fixed by immersion and after a post-mortem delay of >17 h (Impagnatiello *et al.*, 1998; Guidotti *et al.*, 2000) or <10 h followed by embedding in paraffin (Pérez-García *et al.*, 2001). The scant labeling of human cortical pyramidal neurons may thus reflect degradation of immunoreactivity in the samples.

Most Neurons of the Striatum, Thalamus, Brainstem and Cerebellum Contain Reelin

To our knowledge, this is the first report of Reelin protein localization in subcortical regions of primates, and the first, outside the cerebellum, for any adult mammal (Miyata *et al.*, 1996; Pesold *et al.*, 1998).

In situ hybridization studies of Reelin mRNA in adult mice constitute the only, if limited, reference for comparison with the present study (Ikeda and Terashima, 1997; Schiffmann *et al.*, 1997; Alcántara *et al.*, 1998). It seems that the macaque brain contains Reelin protein in all the subcortical cell groups that are equivalent to those hybridizing for Reelin mRNA in adult mice, but, in addition, it also contains Reelin protein in many other regions and neuronal types that do not hybridize Reelin mRNA in mice. An important caveat, however, is that these interspecies differences may be in part only apparent, because the

hybridization experiments in mice were carried out using digoxigenin-labeled riboprobes that may be not sensitive enough for detecting the low levels of mRNA usual in adult brain cells (Hockfield *et al.*, 1993).

Subcortical cell groups labeled in both adult mice and macaque monkeys include the diagonal band of Broca, the amygdala, the pretectum and the anterior olivary nuclei. Nevertheless, hybridization in these regions was reportedly weak, and limited to a few neurons in mice (Alcántara *et al.*, 1998), whereas immunolabeling is robust and widespread in macaque monkeys. Reelin-positive cell groups in macaque monkeys with Reelin mRNA-negative equivalents in adult mice include the striatum, globus pallidus, all the nuclei of the dorsal thalamus, and hypothalamus. One should, however, note that some of these nuclei, such as the striatum and hypothalamic nuclei, do hybridize Reelin mRNA during development (Schiffmann *et al.*, 1997; Alcántara *et al.*, 1998). No mRNA data are available for caudal brainstem nuclei in adult rodents. Interestingly, we show here that the neurons of the inferior olivary, facial and trigeminal nuclei, whose cytoarchitecture is disrupted in reeler mice (Goffinet, 1983; Goffinet *et al.*, 1984a,b), are heavily PReln-ir in adult primates.

The somata of granule cells of the cerebellar cortex (Miyata *et al.*, 1996; Pesold *et al.*, 1998) and the terminal neuropil of their axons (the molecular layer) are heavily Reelin-immunoreactive in rodents (Miyata *et al.*, 1996; Pesold *et al.*, 1998) and macaques (present results). In contrast, the Purkinje cells in the macaque are conspicuously immunoreactive, while their rodent counterparts do not show Reelin messenger or protein either in adults or during development (Ogawa *et al.*, 1995; Miyata *et al.*, 1996; Schiffmann *et al.*, 1997; Alcántara *et al.*, 1998; Pesold *et al.*, 1998).

Inter-species Differences in the Reelin-containing Neuronal Populations

At present, rats are the only other mammals for which extensive Reelin protein mapping in the adult brain is available (Miyata *et al.*, 1996; Pesold *et al.*, 1998). In comparison, our observations in macaques suggest a vast increase in the number of cells and circuits that may be under the direct influence of Reelin in the primate lineage. For a number of reasons, we believe that the inter-order difference is genuine, and cannot be explained away as spurious labeling or antibody cross-reactivity in macaques. First, we obtained similar results with two different, well-characterized monoclonal IgGs that are directed to closely adjacent but non-overlapping amino acid sequences in the F-spondin-like region of Reelin (De Bergeyck *et al.*, 1998; Utsunomiya-Tate *et al.*, 2000; Ichihara *et al.*, 2001) that is critical for protein function (Ogawa *et al.*, 1995; Del Río *et al.*, 1997; Nakajima *et al.*, 1997; Borrell *et al.*, 1999; Utsunomiya-Tate *et al.*, 2000; Quattrocchi *et al.*, 2002). These two antibodies have high affinity for binding the full-length and processed forms of the protein in rodents and primates (De Bergeyck *et al.*, 1998; Impagnatiello *et al.*, 1998; Lacor *et al.*, 2000; Hong *et al.*, 2000). It is very unlikely that the two monoclonal IgGs would react with a protein other than Reelin. Second, omission of the primary antibody yielded no labeling. Third, Rodríguez and colleagues (Rodríguez *et al.*, 2000) reported identical immunolabeling in the isocortical pyramidal cells in three further different Old World primate species: baboon (*Papio papio*), patas monkey (*Erythrocebus pata*) and stump-tailed macaque (*Macaca artoides*), consistent with our observations in *Macaca nemestrina* and *Macaca mulatta*. Although these authors interpreted the PReln-ir labeling as perisomatic axon terminals, their data together with the present data from two additional species of macaque monkeys, imply a widespread expression of Reelin in the primate cerebral cortex.

From a broader perspective, Reelin immunolabeling differences in particular neuronal types of primates and rodents are in consonance with recent evidence for large quantitative differences between different mammals in the mRNA expression and protein levels of numerous genes in equivalent brain regions (Enard *et al.*, 2002). Moreover, a growing number of biochemical/morphological neuronal phenotypes specific to primates have been identified in recent years (DeFelipe, 1997; Elston *et al.*, 2001; González-Albo *et al.*, 2001; Letinic *et al.*, 2002). Together with those reports, the present findings emphasize the relevance of studies focused in the primate brain.

Reelin Function in the Adult Primate Brain

Since its identification in 1995 (D'Arcangelo *et al.*, 1995), Reelin has been investigated mainly as a protein involved in neurodevelopmental mechanisms. In the embryonic brain, Reelin is believed to control neuroblast positioning through the regulation of cell-to-cell adhesion. There is evidence that Reelin may exert this function acting as an intercellular signaling molecule [for recent reviews, see Aboitiz *et al.* (Aboitiz *et al.*, 2001) or Rice and Curran (Rice and Curran, 2001)]. As such, Reelin is secreted, binds to receptors, and triggers several potential transduction pathways in target cells (Derer *et al.*, 2001; Rice and Curran, 2001). The best characterized of these pathways includes binding to very low density lipoprotein receptor and ApoE receptor 2, resulting in an internalization of Reelin and activation of a tyrosine kinase cascade that, in turn, phosphorylates the cytoplasmic adapter protein Disabled-1 (Dab-1) (D'Arcangelo *et al.*, 1999; Hiesberger *et al.*, 1999; Trommsdorff *et al.*, 1999). Parallel, although less clearly delineated, pathways have been proposed that involve binding to integrin $\alpha 3\beta 1$ receptor (Anton *et al.*, 1999; Dulabon *et al.*, 2000), or to cadherin-related neuronal receptors (Senzaki *et al.*, 1999). In the embryonic cerebral isocortex, Reelin-mediated intercellular signaling may be crucial, for example, in the genesis of the inside-out neurogenetic gradient of neurons (Gleeson and Wash, 2000; Rice and Curran, 2001; Magdaleno *et al.*, 2002). In this case, Reelin synthesized and secreted to the extracellular matrix by the Cajal–Retzius cells of the marginal zone (Ogawa *et al.*, 1995) would interact with receptors in cortical plate migrating neuroblasts that do not synthesize Reelin (D'Arcangelo *et al.*, 1995; Schiffmann *et al.*, 1997; Alcántara *et al.*, 1998), but do express Dab-1 (Howell *et al.*, 1997; Rice *et al.*, 1998).

There is now ample evidence that Reelin is also widely present in the adult brain (Schiffmann *et al.*, 1997; Alcántara *et al.*, 1998; Pesold *et al.*, 1998, 1999; Rodríguez *et al.*, 2000; Pappas *et al.*, 2002; present results); however, its function/s there are still elusive. As in development, Reelin is secreted to the extracellular space (Pappas *et al.*, 2002). It has been suggested that Reelin could be involved in the modulation of synaptic plasticity acting as an intercellular signaling molecule between interneurons and pyramidal cells through a Dab-1-mediated pathway (Pesold *et al.*, 1998, 1999; Rodríguez *et al.*, 2000). This conclusion was based on observations in rodents that (a) Reelin protein and mRNA (as detected with digoxigenin-labeled riboprobes) were present in several cortical interneuron populations, (b) they were absent in most (but not all) pyramidal cells, and (c) the Dab-1 adapter protein is present in pyramidal cells and some interneurons (Pesold *et al.*, 1998; Rodríguez *et al.*, 2000).

Our observations in macaques show, in contrast, that virtually all the pyramidal cells and numerous interneurons contain

substantial amounts of Reelin in their secretory pathway organelles. The most straightforward interpretation is that both pyramidal cells and interneurons synthesize and secrete Reelin in macaques. It is thus difficult to envision that the main role of this protein is to act as an intercellular signaling molecule between the two neuronal populations as has been proposed (Pesold *et al.*, 1998, 1999; Rodríguez *et al.*, 2000). Admittedly, such a role cannot conclusively ruled out because there is a small population of interneurons that seem not to contain Reelin.

Although we favor the conclusion that all Reelin-immunoreactive neurons synthesize Reelin, lack of mRNA data in primates still leaves open the possibility that only SReln-ir cortical interneurons synthesize Reelin (Pesold *et al.*, 1998, 1999; Rodríguez *et al.*, 2000). To account for our observations, however, this would require that pyramidal cells (and many other subcortical PReln-ir cells as well) would somehow internalize and accumulate large amounts of the protein in their Golgi apparatus. There are suggestions that secreted Reelin may be internalized after binding α3β1 integrin (Dulabon *et al.*, 2000), and it is known that the Golgi apparatus is involved in receptor-mediated endocytosis and subsequent processing of some proteins (Gonatas *et al.*, 1994). Nevertheless, even if such a mechanism could explain labeling in PReln-ir cortical pyramids, which are adjacent to numerous SReln-ir interneurons, it is more difficult to explain the widespread PReln-ir observed in structures like the striatum, thalamus, etc., that lack SReln-ir neurons (Table 1). Furthermore, since published studies have found no Reelin protein in most cortical pyramids in other mammals (Pesold *et al.*, 1998; Martínez-Cerdeño and Clascá, 2002), the hypothesized internalization–accumulation mechanism would still be largely specific to primates. *In situ* hybridization studies in primates using sensitive riboprobes should definitively settle this issue in the future.

Recent evidence that Reelin itself is a serine-protease in the extracellular matrix (Quattrocchi *et al.*, 2002) indicates that Reelin may well play functional roles other than in intercellular signaling. Secreted Reelin could be involved in the rapid proteolytic modulation of adhesive forces between pre- and postsynaptic elements, thus modulating the efficiency of synaptic transmission at the local level (Quattrocchi *et al.*, 2002). Binding to integrins (Dulabon *et al.*, 2000; Rodríguez *et al.*, 2000) would be important for stabilizing the secreted protein in local dendritic domains. These observations have led to the proposal that proteolytic regulation of synaptic transmission may be a major role for Reelin in the adult (Quattrocchi *et al.*, 2002). Our finding of Reelin in most cell types of the adult macaque brain, and its localization in somata, axons and neuropil appear to be consistent with such a role.

Notes

The authors wish to thank Dr Stephen Noctor for critical review of an earlier version of the manuscript, as well as Dr André Goffinet for the gift of the Reelin 142 antibody, Dr Masaru Ogawa for the CR 50 antibody, and Dr Estrella Rausell for the *Macaca mulatta* tissue. Support was provided by the Ministries of Health (FIS 98/0286) and of Science and Technology (DGESIC PB 97/015, BMC2001-0623) to F.C. and (DGESIC PB98-0064) to C.C. V.M. is the recipient of a predoctoral fellowship from Fondo de Investigación Sanitaria (BEFI 99/9160).

Address correspondence to Dr Francisco Clascá, Neurodevelopmental Unit, Department of Morphology, Autónoma University School of Medicine, Ave. Arzobispo Morcillo 4, Madrid, Spain E-28029. Email: francisco.clasca@uam.es.

References

Aboitiz F, Morales D, Montiel J (2001) The inverted neurogenetic gradient of the mammalian isocortex: development and evolution. Brain Res Rev 38:129–139.

Alcántara S, Ruiz M, D'Arcangelo G, Ezan F, de Lecea L, Curran T, Sotelo C, Soriano E (1998) Regional and cellular patterns of Reelin mRNA expression in the forebrain of the developing and adult mouse. J Neurosci 18:7779–7799.

Anton ES, Kreidberg JA, Rakic P (1999) Distinct functions of alpha3 and alpha (v) integrin receptors in neuronal migration and laminar organization of the cerebral cortex. Neuron 22:277–289.

Blinkov S, Glezer I (1968) The human brain in figures and tables. A quantitative handbook. New York: Plenum.

Borrell V, Del Rio JA, Alcántara S, Derer M, Martinez A, D'Arcangelo G, Nakajima K, Mikoshiba K, Derer P, Curran T, Soriano E (1999) Reelin regulates the development and synaptogenesis of the layer-specific entorhino-hippocampal connections. J Neurosci 19:1345–1358.

Carmichael ST, Clugnet MC, Price JL (1994) Central olfactory connections in the macaque monkey. J Comp Neurol. 346:403–434.

Caviness VS, Crandall JE, Edwards MA (1988) The Reeler malformation. Implications for neocortical histogenesis. In: Cerebral cortex, vol. 7 (Peters A, Jones EG, eds), pp. 59–89. New York: Plenum.

D'Arcangelo G., Miao GG, Chen SC, Soares HD, Morgan JI, Curran T (1995) A protein related to extracellular matrix proteins deleted in the mouse mutant reeler. Nature 374:719–723.

D'Arcangelo G, Nakajima K, Miyata T, Ogawa M, Mikoshiba K, Curran T. (1997) Reelin is a secreted glycoprotein recognized by the CR-50 monoclonal antibody. J Neurosci 17:23–31.

D'Arcangelo G, Homayouni R, Keshvara L, Rice DS, Sheldon M, Curran T (1999) Reelin is a ligand for lipoprotein receptors. Neuron 24: 471–479.

De Bergeyck V, Naerhuyzen B, Goffinet AM, Lambert de Rouvroit CA (1998) Panel of monoclonal antibodies against Reelin, the extracellular matrix protein defective in reeler mutant mice. J Neurosci Methods 82:17–24.

De Camilli P, Moretti M, Donini SD, Walter U, Lohman SM (1986) Heterogeneous distribution of the camp receptor protein RII in the nervous system: evidence for its intracellular accumulation on microtubules, microtubule-organizing centers, and in the area of the Golgi complex. J Cell Biol 103:189–203.

DeFelipe J (1997) Types of neurons, synaptic connections and chemical characteristics of cells immunoreactive for calbindin-D28K, parvalbumin and calretinin in the neocortex. J Chem Neuroanat 14:1–19.

Del Rio JA, Martinez A, Fonseca M, Auladell C, Soriano E (1995) Glutamate-like immunoreactivity and fate of Cajal–Retzius cells in the murine cortex as identified with calretinin antibody. Cereb Cortex 5:13–21.

Del Rio JA, Heimrich B, Supèr H, Boreell V, Frotscher M, Soriano E (1996) Differential survival of Cajal–Retzius cells in organotypic cultures of hippocampus and neocortex. J Neurosci 16:6896–6907.

Del Rio JA, Heimrich B, Borrell V, Forster E, Drakew A, Alcántara S, Nakajima K, Miyata T, Ogawa M, Mikoshiba K, Derer P, Frotscher M, Soriano E (1997) A role for Cajal–Retzius cells and Reelin in the development of hippocampal connections. Nature 38:70–74.

Derer P, Derer M, Goffinet A (2001) Axonal secretion of Reelin by Cajal–Retzius cells: evidence from comparison of normal and Reln (Orl) mutant mice. J Comp Neurol 440:136–143.

Dulabon L, Olson EC, Taglienti MG, Eisenhuth S, McGrath B, Walsh CA, Kreidberg JA, Anton ES (2000) Reelin binds α3β1 integrin and inhibits neuronal migration. Neuron 27:33–44.

Elston GN, Benavides-Piccione R, DeFelipe J. (2001) The pyramidal cell in cognition: a comparative study in human and monkey. J Neurosci 21:RC163.

Enard W, Khaitovich P, Klose J, Zollner S, Heissig F, Giavalisco P, Nieselt-Struwe K, Muchmore E, Varki A, Ravid R, Doxiadis GM, Bontrop RE, Paabo S (2002) Intra- and interspecific variation in primate gene expression patterns. Science 296:340–343.

Fatemi SH, Earle JA, McMenomy T (2000) Hippocampal CA4 Reelin-positive neurons. Mol Pschiatry 5:71.

Gleeson JG, Walsh CA (2000) Neuronal migration disorders: from genetic diseases to developmental mechanisms. Trends Neurosci 23:352–359.

Goffinet AM (1983) The embryonic development of the inferior olivary complex in normal and reeler mutant mice. J Comp Neurol 219:10–24.

Goffinet AM (1984a) Events governing organization of postmigratory

neurons: studies on brain development in normal and reeler mice. Brain Res Rev 7:261–296.
Goffinet AM (1984b) Abnormal development of the facial nerve nucleus in the reeler mutant mice. J Anat 138:207–215.
Gonatas NK (1994) Contributions to the physiology and pathology of the Golgi apparatus. Am J Pathol 145:751–761.
González-Albo MC, Elston GN, DeFelipe J (2001) The human temporal cortex: characterization of neurons expressing nitric oxide synthase, neuropeptides and calcium-binding proteins, and their glutamate receptor subunit profiles. Cereb Cortex 11:1170–1181.
Guidotti A, Auta J, Davis JM, Gerevini VD, Dwivedi Y, Grayson DR, Impagnatiello F, Pandey G, Pesold C, Sharma R, Uzunov D, Costa E (2000) Decrease in Reelin and glutamic acid decarboxylase 67 (GAD67) expression in schizophrenia and bipolar disorder: a postmortem brain study. Arch Gen Psychiatry 57:1061–1069.
Heymann R, Kallenbach S, Alonso S, Carroll P, Mitsiadis TA (2001) Dynamic expression patterns of the new protocadherin families CNRs and Pcdh-gamma during mouse odontogenesis: comparison with Reelin expression. Mech Dev 106:181–184.
Hiesberger T, Trommsdorff M, Howell BW, Goffinet A, Mumby MC, Cooper JA, Herz J (1999) Direct binding of Reelin to VLDL receptor and ApoE receptor 2 induces tyrosine phosphorylation of disabled-1 and modulates tau phosphorylation. Neuron 24:481–489.
Hockfield S, Carlson S, Evans C, Levitt P, Pintar J, Silberstein L (1993) Selected methods for antibody and nucleic acid probes. Plainview, NY: Cold Spring Harbor Laboratory Press.
Hong SE, Shugart YY, Huang DT, Shahwan SA, Grant PE, Hourihane JO, Martin ND, Walsh CA (2000) Autosomal recessive lissencephaly with cerebellar hypoplasia is associated with human RELN mutations. Nat Genet 26:93–96.
Howell BW, Hawkes R, Soriano P, Cooper JA (1997) Neuronal position in the developing brain is regulated by mouse disabled-1. Nature 389:733–737.
Ichihara H, Jingami H, Toh H (2001) Three novel repetitive units of Reelin. Brain Res Mol Brain Res 97:190–193.
Ikeda Y, Terashima T (1997) Expression of Reelin, the gene responsible for the reeler mutation, in embryonic development and adulthood in the mouse. Dev Dyn 210:157–172.
Impagnatiello F, Guidotti AR, Pesold C, Dwivedi Y, Caruncho H, Pisu MG, Uzunov DP, Smalheiser NR, Davis JM, Pandey GN, Pappas GD, Tueting P, Sharma RP, Costa E (1998) A decrease of Reelin expression as a putative vulnerability factor in schizophrenia. Proc Natl Acad Sci USA 95:15718–15723.
Jossin Y, Goffinet AM (2001) Reelin does not directly influence axonal growth. J Neurosci 21:RC183 (1–4).
Klar A, Baldassare M, Jessell TM (1992) F-spondin: a gene expressed at high levels in the floor plate encodes a secreted protein that promotes neural cell adhesion and neurite extension. Cell 69:95–110.
Lacor PN, Grayson DR, Auta J, Sugaya I, Costa E, Guidotti A (2000) Reelin secretion from glutamatergic neurons in culture is independent from neurotransmitter regulation. Proc Natl Acad Sci USA 97:3556–3561.
Lambert de Rouvroit C, de Bergeyck V, Cortvrindt C, Bar I, Eeckhout Y, Goffinet AM (1999) Reelin, the extracellular matrix protein deficient in reeler mutant mice, is processed by a metalloproteinase. Exp Neurol 156:214–217.
Letinic K, Zencu R, Rakic P (2002) Origin of GABAergic neurons in the human neocortex. Nature 417:645–649.
Magdaleno S, Keshvara L, Curran T (2002) Rescue of ataxia and preplate splitting by ectopic expression of Reelin in reeler mice. Neuron 33:573–586.
Marin-Padilla M (1998) Cajal–Retzius cells and the development of the neocortex. Trends Neurosci 21:64–71.
Martínez-Cerdeño and Clascá F (2002) Reelin immunoreactivity in the adult neocortex: a comparative study in rodents, carnivores and non-human primates. Brain Res Bull 57:485–488.
Meyer G, Goffinet AM (1998) Prenatal development of Reelin-immunoreactive neurons in the human neocortex. J Comp Neurol 397:29–40.
Miyata T, Nakajima K, Aruga J, Takahashi S, Ikenaka K, Mikoshiba K, Ogawa M (1996) distribution of a reeler gene-related antigen in a developing cerebellum: an immunohistochemical study with an allogenic antibody CR-50 in normal and reeler mice. J Comp Neurol 372:215–228.
Nakajima K, Mikoshiba K, Miyata T, Kudo C, Ogawa M (1997) Disruption of hippocampal development *in vivo* by CR-50 mAb against Reelin. Proc Natl Acad Sci USA 94:8196–8201.
Ogawa M, Miyata T, Nakajima K, Yagyu K, Seike M, Ikenaka K, Yamamoto H, Mikoshiba K (1995) The reeler gene-associated antigen on Cajal–Retzius neurons is a crucial molecule for laminar organization of cortical neurons. Neuron 14:899–912.
Pappas GD, Kriho V, Pesold C (2002) Reelin in the extracellular matrix and dendritic spines of the cortex and hippocampus: a comparison between wild type and heterozygous reeler mice by immunoelectron microscopy. J Neurocytol 20:413–425.
Pérez-García CG, Gonzalez-Delgado FJ, Suarez-Sola ML, Castro-Fuentes R, Martin-Trujillo JM, Ferres-Torres R, Meyer G (2001) Reelin-immunoreactive neurons in the adult vertebrate pallium. J Chem Neuroanat 21:41–51.
Pesold C, Pisu M, Impagnatiello F, Uzunov DP, Caruncho HJ (1998) Simultaneous detection of glutamic acid decarboxylase and Reelin mRNA in adult rat neurons using *in situ* hybridization and immunofluorescence. Brain Res Brain Res Protoc 3:155–160.
Pesold C, Liu WS, Guidotti A, Costa E, Caruncho HJ (1999) Cortical bitufted, horizontal, and Martinotti cells preferentially express and secrete Reelin into perineuronal nets, nonsynaptically modulating gene expression. Proc Natl Acad Sci USA. 96:3217–3222.
Peters A, Palay SL, Webster D (1991) The fine structure of the nervous system, 3rd edn. New York: Oxford University Press.
Phelps PE, Rich R, Dupuy-Davies S, Ríos Y, Wong T (2002) Evidence for a cell-specific action of Reelin in the spinal cord. Dev Biol 244:180–198.
Quattrocchi CC, Wannenes F, Persico AM, Ciafre SA, D'Arcangelo G, Farace MG, Keller F (2002) Reelin is a serine protease of the extracellular matrix. J Biol Chem 277:303–309.
Rice DS, Curran T (2001) Role of the Reelin signaling pathway in central nervous system development. Annu Rev Neurosci 24:1005–1039.
Rice DS, Sheldon M, D'Arcangelo G, Nakajima K, Goldowitz D, Curran T (1998) Disabled-1 acts downstream of Reelin in a signaling pathway that controls laminar organization in the mammalian brain. Development 125:3719–3729.
Rodríguez MA, Pesold C, Liu WS, Kriho V, Guidotti A, Pappas GD, Costa E (2000) Colocalization of integrin receptors and Reelin in dendritic spine postsynaptic densities of adult nonhuman primate cortex. Proc Natl Acad Sci USA 97:3550–3555.
Rosene DL, Van Hoesen GW (1987) The hippocampal formation of the primate brain. In: Cerebral cortex, vol. 6 (Jones EG, Peters A, eds), pp. 345–455. New York: Plenum.
Schiffmann SN, Bernier B, Goffinet AM (1997) Reelin mRNA expression during mouse brain development. Eur J Neurosci 9:1055–1071.
Senzaki K, Ogawa M, Yagi T (1999) Proteins of the CNR family are multiple receptors for Reelin. Cell 99:635–647.
Smalheiser NR, Costa E, Guidotti A, Impagnatiello F, Auta J, Lacor P, Kriho V, Pappas GD (2000) Expression of Reelin in adult mammalian blood, liver, pituitary pars intermedia, and adrenal chromaffin cells. Proc Natl Acad Sci USA 97:1281–1286.
Trommsdorff M, Gotthardt M, Hiesberger T, Shelton J, Stockinger W, Nimpf J Hammer RE, Richardson JA, Herz J (1999) Reeler/Disabled-like disruption of neuronal migration in knockout mice lacking the VLDL receptor and ApoE receptor 2. Cell 97:689–701.
Utsunomiya-Tate N, Kubo K, Tate S, Kainosho M, Katayama E, Nakajima K, Mikoshiba K (2000) Reelin molecules assemble together to form a large protein complex, which is inhibited by the function-blocking CR-50 antibody. Proc Natl Acad Sci USA 97:9729–9734.
Zecevic N, Rakic P (2001) Development of layer I neurons in the primate cerebral cortex. J Neurosci 21:5607–5619.